Eur J Nucl Med Mol Imaging (2017) 44:876–885
DOI 10.1007/s00259-016-3588-x

ORIGINAL ARTICLE

Left ventricular function in response to dipyridamole stress: head-to-head comparison between ^{82}Rubidium PET and ^{99m}Tc-sestamibi SPECT ECG-gated myocardial perfusion imaging

Maria Clementina Giorgi[1] · Jose Claudio Meneghetti[1] · Jose Soares Jr.[1] · Marisa Izaki[1] · Andréa Falcão[1] · Rodrigo Imada[1] · William Chalela[1] · Marco Antonio de Oliveira[1] · Cesar Nomura[1] · Hein J. Verberne[2]

Received: 15 August 2016 / Accepted: 24 November 2016 / Published online: 16 December 2016

Abstract
Purpose Myocardial perfusion imaging (MPI) with ^{99m}Tc-sestamibi (sestamibi) SPECT and rubidium-82 (^{82}Rb) PET both allow for combined assessment of perfusion and left ventricular (LV) function. We sought to compare parameters of LV function obtained with both methods using a single dipyridamole stress dose.
Materials and methods A group of 221 consecutive patients (65.2 ± 10.4 years, 52.9% male) underwent consecutive sestamibi and ^{82}Rb MPI after a single dipyridamole stress dose. Sestamibi and ^{82}Rb summed rest (SRS), stress (SSS) and difference (SDS) scores, and LV end-diastolic (EDV) and end-systolic (ESV) volumes and left ventricular ejection fraction (LVEF) were compared.
Results Bland-Altman analysis showed that with increasing ESV and EDV the difference between the two perfusion tracers increased both at rest and post-stress. The mean difference in EDV and ESV between the two perfusion tracers at rest could both be independently explained by the ^{82}Rb SDS and the sestamibi SRS. The combined models explained approximately 30% of the variation in these volumes between the two perfusion tracers ($R^2 = 0.261$, $p = 0.005$; $R^2 = 0.296$, $p < 0.001$, for EDV and ESV respectively). However, the mean difference in LVEF between sestamibi and ^{82}Rb showed no significant trend post-stress ($R^2 = 0.001$, $p = 0.70$) and only a modest linear increase with increasing LVEF values at rest ($R^2 = 0.032$, $p = 0.009$).
Conclusions Differences in left ventricular volumes between sestamibi and ^{82}Rb MPI increase with increasing volumes. However, these differences did only marginally affect LVEF between sestamibi and ^{82}Rb. In clinical practice these results should be taken into account when comparing functional derived parameters between sestamibi and ^{82}Rb MPI.

Keywords Myocardial perfusion imaging · Single-photon emission computed tomography · Positron emission tomography · Stress ejection fraction

✉ Hein J. Verberne
h.j.verberne@amc.uva.nl

1 Department of Radiology and Nuclear Medicine and Molecular Imaging Service - Heart Institute of the University of São Paulo Medical School, São Paulo, Brazil

2 Department of Nuclear Medicine, Academic Medical Center, University of Amsterdam, P.O. Box 22700, 1100 DE Amsterdam, The Netherlands

Introduction

Myocardial single-photon emission computed tomography (SPECT) using technetium-99 m (^{99m}Tc) labeled tracers is a widespread imaging modality for assessing myocardial perfusion and left ventricular function. However, its power to diagnose and evaluate the extent of disease in patients who are suspected for coronary artery disease (CAD) or in those with already established CAD is mainly hampered by its somewhat low specificity, limited spatial resolution, and difficulties for absolute quantification. To overcome these limitations of SPECT-assessed myocardial perfusion, attempts have been made with a varying degree of success, including the use of attenuation correction and scatter correction, new crystal and collimator systems, advanced processing software [1, 2]. However, the majority of these (technical) SPECT related limitations can be overcome with positron emission computed tomography (PET).

Cardiac PET myocardial perfusion imaging is being performed clinically with tracers such as N13-ammonia (^{13}N-NH_3) and rubidium-82 (^{82}Rb). Besides having a more favorable radiation exposure profile [3], PET myocardial perfusion provide improved image contrast and allows for quantitative measurements of myocardial blood flow and coronary flow reserve. In addition, PET myocardial perfusion has a high diagnostic accuracy [4–7]. Important to realize is that the spatial resolution of PET images is directly related to the positron range. The higher the energy of the emitted positron, the longer it travels away from the source before annihilation and the worse the resolution of the imaged target will be. In other words the shorter the positron range, the better the spatial resolution and image quality (^{18}F: 1.03 mm; ^{13}N-NH_3: 2.53 mm; ^{15}O-water: 4,4 mm; and ^{82}Rb: 8,6 mm) [8]. Because of its relatively long positron range the spatial resolution and image quality of ^{82}Rb PET is not so superior to SPECT.

Beyond the physical characteristics, which provide better image quality and shorter examination duration, some PET tracers allow for the assessment of left ventricular function during or directly after the stress test. In contrast, SPECT stress imaging is usually performed with some delay after completion of stress testing. During this delay, left ventricular hemodynamic and functional changes that occurred during stress may recover partially or completely to baseline, potentially leading to an underestimation of disease severity.

Differences among studies obtained with ^{82}Rb PET imaging and SPECT tracers have been described. A study comparing the sensitivity, specificity, and accuracy of thallium-201 and ^{82}Rb after a singular stress test analyzed relative perfusion but did not address possible differences in left ventricular function [5]. There are data that show that there are intra-individual differences in relative perfusion and functional left ventricular parameters between sestamibi SPECT and ^{82}Rb PET [4]. However, these results are hampered by the fact that the data were obtained with separate and sequential stress tests. Therefore, the aim of this study was to compare left ventricular function obtained with sestamibi SPECT and ^{82}Rb PET using a single stress test and to verify whether the presence of perfusion defects is associated with differences in left ventricular function in response to stress.

Materials and methods

Patient population

The study included 221 consecutive patients who were clinically referred for pharmacological stress myocardial perfusion scintigraphy. The study was approved by the local institutional review board and conducted according to the principles of the International Conference on Harmonization–Good Clinical Practice. All patients provided written informed consent.

Patients were instructed to fast for 4 h, not to consume caffeine for 24 h and, when possible, to stop oral beta-blockers and calcium channel blockers for 3 days, theophylline or theophylline-containing medication for 36 h, and long-acting nitrates for 6 h before the examinations.

Study protocol

Patients underwent ^{82}Rb PET and sestamibi SPECT using a single stress test (Fig. 1). ECG was continuously monitored; blood pressure was measured before dipyridamole infusion, at the second minute, at the end of infusion, and after 10 min of dipyridamole infusion.

Two low-dose CT scans were performed after normal end-expiration before rest ^{82}Rb dose and after stress ^{82}Rb images to correct for attenuation of the photons. Rest and stress ^{82}Rb images (gated to the patients' ECG) were acquired in a Gemini-TOF 64 slice system (Philips Medical Systems, Cleveland, OH, USA) in list-mode format.

Rest and stress sestamibi acquisitions were ECG-gated obtained on a Cardio 1 MD system without attenuation correction (Philips Medical Systems, Cleveland, OH, USA) using a step-and-shoot protocol. Sixty- four images were acquired in a semicircular orbiter (25 s per projection for rest and 20 s for stress studies) using a 64×64 matrix and eight frames per cardiac cycle using low-energy, high-resolution collimators, 140 keV photopeak, and a 15% window.

Image reconstruction and processing

SPECT images were reconstructed using iterative ordered subset expectation maximization (OSEM) with 12 iterations and a 0.65 Butterworth filter.

PET images were reconstructed using a 3-dimensional row-action maximum likelihood algorithm (3D-RAMLA) with three iterations and 33 subsets. ^{82}Rb images were evaluated for spatial misalignment between CT and PET and were manually corrected if necessary.

After reconstruction, both SPECT and PET images were analyzed using the same commercial software package (Cedars Sinai QPET and 4D QGS, version 2012.2). With this package end-diastolic (EDV), end-systolic (ESV) left ventricular volumes at rest and stress (in mL), LVEF at rest and stress (in percentage units) were determined for both perfusion tracers.

Image interpretation

Reconstructed images were reoriented according to the heart axes and visually reviewed by two experienced observers

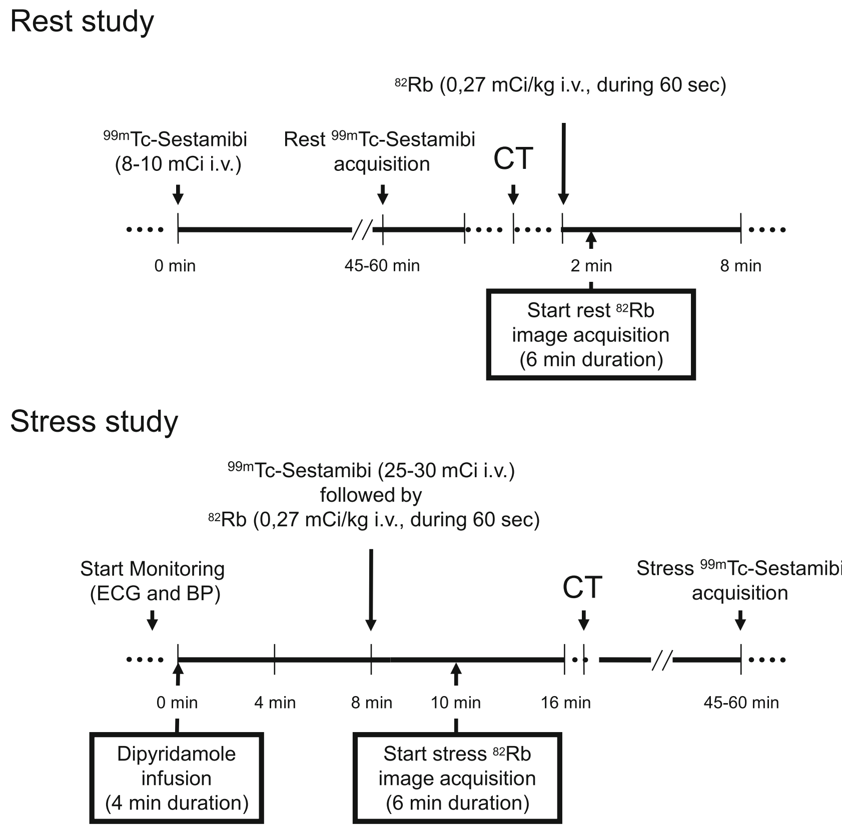

Fig. 1 Sestamibi SPECT and ^{82}Rb PET using a single stress test

unaware of clinical data. A third opinion was obtained when consensus was not reached. Relative perfusion was evaluated using a 5-point score (0 = normal, 1 = mildly decreased uptake, 2 = moderate, 3 = severely decreased uptake, 4 = no uptake) and a standard 17-segment model [9].

Summed scores obtained from rest (SRS) and stress (SSS) images as well as the difference score (SDS) between stress and rest were calculated for both SPECT and PET.

Statistical analysis

All continuous variables are expressed as mean ± standard deviation. Differences in mean values were compared with a (paired) student *t*-test. Bland-Altman analysis was used to compare the differences between SPECT and PET in perfusion and functional left ventricular parameters post-stress and at rest.

Multivariate linear regression analysis was performed to determine possible independent predictors (i.e. age, gender, body mass index, delay between stress injection, SSS, SRS, and SDS) of the mean differences between SPECT and PET derived functional parameters (i.e. LEVF, ESV, and EDV). The overall goodness-of-fit for each model was expressed as the adjusted R^2. The F-test was used to assess whether a model explained a significant proportion of the variability. A *p*-value < 0.05 was considered to indicate a statistical significance. All statistical analyses were performed using the software package SPSS, version 22.0.0.2 (IBM® SPSS® Statistics, Chicago, IL, USA).

Results

Study population

A group of 221 consecutive patients (65.2 ± 10.4 years, 52.9% male) underwent consecutive ^{82}Rb and sestamibi MPI after a single dipyridamole stress dose. The majority of patients was referred for the primary evaluation of chest pain (angina or equivalent, $n = 122$; 55.2%) or the evaluation of known coronary artery disease [$n = 87$; 39.4%, including those with a previous PTCA ($n = 26$) and those with a previous CABG ($n = 22$)]. Only a minority of patients was referred in the context of preoperative risk evaluation ($n = 12$, 5.4%). Demographic and hemodynamic data of this population are displayed in Table 1.

Differences in perfusion

Although there were small but statistical significant differences in both SRS and SDS, there was no statistical significant difference in SSS between the sestamibi and

Table 1 Demographic data and hemodynamic response to pharmacological stress with dipyridamole in the study population (*n* = 221 patients)

Age, years (mean ± SD)	65.2 ± 10.4
Male sex (n, %)	117 (52.9)
Body mass index	28.4 ± 5.0
Diabetes (%)	99 (44.6)
Hypertension (%)	191 (86.6)
Dyslipidemia (%)	113 (51.2)
Chronic kidney disease (%)	45 (20.4)
Previous infarction (%)	59 (26.9)
Heart failure (%)	30 (13.4)
Smoker/previous smoker (%)	80 (36.1)
Heart rate, beats per minute (mean ± SD)	
rest	65.5 ± 12.7
dipyridamole	78.0 ± 13.8*
Systolic blood pressure, mmHg (mean ± SD)	
rest	142.0 ± 23.3
dipyridamole	141.0 ± 22.60
Diastolic blood pressure, mmHg (mean ± SD)	
rest	77.0 ± 12.17
dipyridamole	74.0 ± 12.72
Rate pressure product (mean ± SD)	
rest	9540.0 ± 2484.8
dipyridamole	11023.0 ± 2730.3*

mean ± SD = mean value ± standard deviation; * $p < 0.05$ rest versus dipyridamole

^{82}Rb images (Table 2). Interestingly, Bland-Altman analysis showed a linear increase in difference between the sestamibi and ^{82}Rb images with increasing mean SSS and SRS (i.e. larger scores for the sestamibi perfusion images with increasing mean values as compared with the ^{82}Rb images) ($R^2 = 0.107$, $p < 0.001$ vs. $R^2 = 0.440$, $p < 0.001$, respectively). For the SDS a reversed pattern between sestamibi and ^{82}Rb images was seen (i.e. lower scores for the sestamibi perfusion images with increasing mean values as compared with the ^{82}Rb images) ($R^2 = 0.306$, $p < 0.001$) (Fig. 2).

Of the total perfusion examinations, 144 were scored as normal (i.e. SSS ≤ 3) on sestamibi SPECT and 135 on ^{82}Rb PET (Table 3). On a group level this resulted in a nonsignificant difference ($p = 0.106$). On an individual patient level this meant that a change in classification from normal to abnormal or vice versa occurred in 39 patients. In 25 patients the score changed from normal on SPECT to abnormal (SSS ≥ 3) on PET and in 14 patients the vice versa took place. Thirty-two patients were reclassified when the analysis was limited to only those patients with a difference in SSS ≥ 2 between SPECT and PET. In 22 patients the score then changed from normal on SPECT to abnormal on PET and in 10 patients the normal PET studies were classified as abnormal on SPECT. Although there were differences in volumes between sestamibi SPECT and ^{82}Rb PET for both normal and abnormal perfusion images the impact of these differences on the difference in LVEF was limited (Table 3).

Table 2 Mean values and standard deviation of the studied parameters obtained for sestamibi and ^{82}Rb studies (*n* = 221)

Parameter	Sestamibi	^{82}Rb	Difference	*p*-value
SRS	3.57 ± 6.61	2.35 ± 4.25	1.22 ± 3.69	<0.001
SSS	4.52 ± 7.48	4.57 ± 6.12	−0.06 ± 4.25	0.808
SDS	0.95 ± 2.39	2.23 ± 3.92	−1.28 ± 3.02	<0.001
Rest LVEF (%)	56.79 ± 15.45	55.16 ± 17.37	1.62 ± 11.13	0.042
Stress LVEF (%)	57.23 ± 16.14	60.57 ± 16.54	−3.39 ± 9.96	<0.001
Rest EDV (mL)	98.96 ± 56.08	87.89 ± 44.23	11.09 ± 21.81	<0.001
Stress EDV (mL)	99.48 ± 57.56	97.72 ± 45.85	1.72 ± 23.4	0.403
Rest ESV (mL)	48.85 ± 48.27	43.42 ± 38.75	5.61 ± 16.51	<0.001
Stress ESV (mL)	49.29 ± 49.44	43.1 ± 9.07	6.24 ± 19.53	<0.001

SRS summed rest score, *SSS* summed stress score, *SDS* summed difference score, *Rest LVEF* left ventricular ejection fraction at rest, *Stress LVEF* stress left ventricular ejection fraction, *Rest EDV* end diastolic volume at rest, *Stress EDV* stress end diastolic volume, *Rest ESV* end systolic volume at rest, *Stress ESV* stress end systolic volume

Differences in functional parameters

The mean difference in LVEF between sestamibi and ^{82}Rb both at stress and at rest was relatively small, but statistically significant (Table 2). For the mean difference in stress LVEF between sestamibi and ^{82}Rb there was no significant trend or bias with increasing LVEF values ($R^2 = 0.001$, $p = 0.70$) (panel A of Fig. 3). Bland-Altman analysis showed a modest but statistically significant linear increase in difference between the sestamibi and ^{82}Rb images with increasing LVEF at rest (i.e. larger LVEF values for the sestamibi perfusion images with increasing mean values as compared with the ^{82}Rb images) ($R^2 = 0.032$, $p = 0.009$) (panel A of Fig. 4).

Also, for ESV and EDV the mean difference between sestamibi and ^{82}Rb both at stress and at rest was relatively small but statistical significant (Table 2). Bland-Altman analysis showed for both ESV and EDV, both at stress and at rest, a linear increase in difference between the sestamibi and ^{82}Rb images with increasing mean ESV and EDV, respectively (i.e. larger scores for the sestamibi perfusion images with increasing mean values as compared with the ^{82}Rb images): EDV at stress $R^2 = 0.252$ ($p < 0.001$) and ESV at stress 0.296 ($p < 0.001$) (panel B and C of Fig. 2) and EDV at rest $R^2 = 0.316$ ($p < 0.001$) and ESV at rest $R^2 = 0.365$ ($p < 0.001$) (panel B and C of Fig. 4).

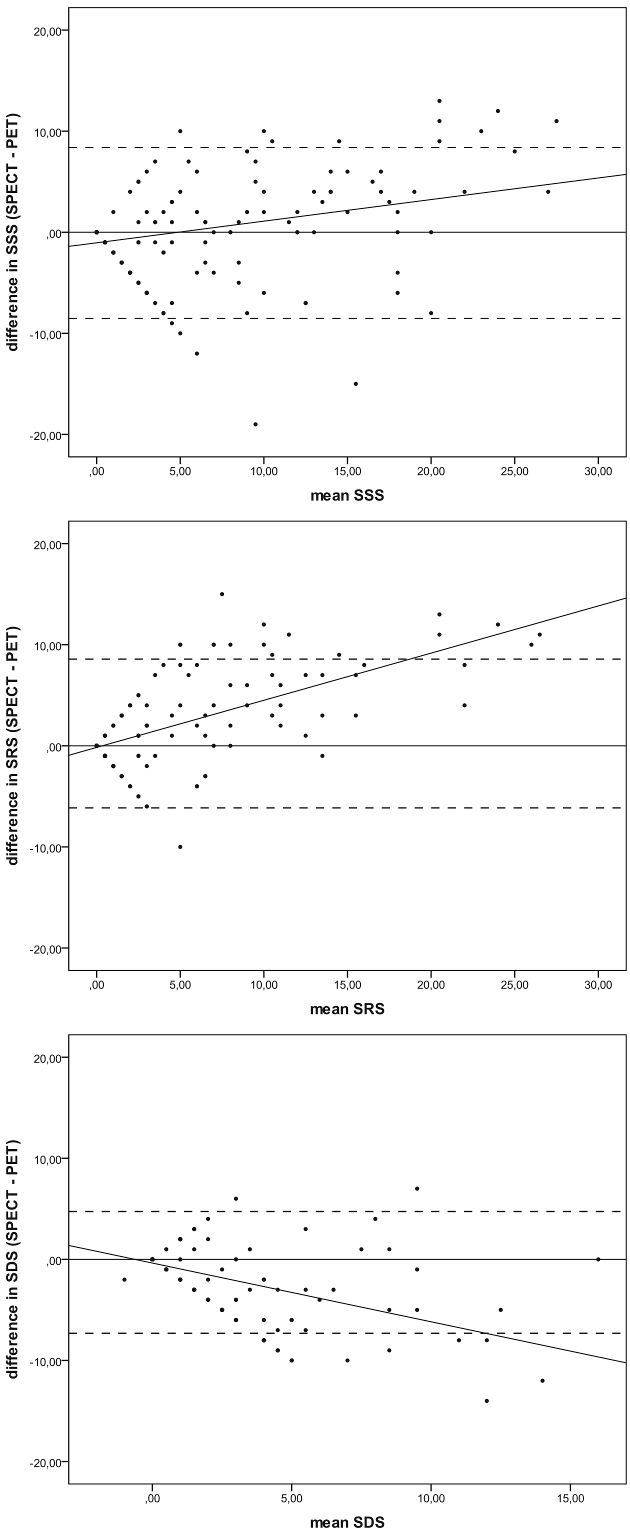

Fig. 2 Bland-Altman plots showing the difference between the SSS (**a**), SRS (**b**), and SDS (**c**) plotted against the mean values of these parameters visually scored on the sestamibi SPECT and ^{82}Rb PET images. Differences were calculated as sestamibi SPECT minus ^{82}Rb PET. The *dashed lines* indicate the 95% limits of agreement of the mean difference and the *solid angular lines* indicates the regression line

Multivariate regression analysis

Multivariate regression analyses showed that the ^{82}Rb SRS, sestamibi SDS, and age were independent predictors of both the mean differences in EDV and ESV on stress images (Table 4). The combined models explained approximately 20% of the variation in the mean difference in EDV and ESV at stress between both perfusion tracers ($R^2 = 0.236$, $p < 0.001$; $R^2 = 0.202$, $p < 0.001$, for EDV and ESV, respectively). The mean difference in EDV and ESV between the two perfusion tracers at rest could both be independently explained by the ^{82}Rb SDS and the sestamibi SRS (Table 5). As for the difference in EDV and ESV at rest the combined models explained approximately 30% of the variation in these volumes between the two perfusion tracers ($R^2 = 0.261$, $p = 0.005$; $R^2 = 0.296$, $p < 0.001$, for EDV and ESV, respectively).

None of the other parameters used (i.e. age, gender, body mass index, delay between stress injection and SSS) were independent predictors for the mean differences in EDV and ESV, nor for stress or rest.

Discussion

This study evaluated the differences in functional data and relative myocardial perfusion imaging between PET and SPECT in a relatively large patient cohort with known or suspected CAD referred for myocardial perfusion scintigraphy. The design of the study enabled us to study these possible differences with a single stress test.

The main findings of this study are that differences in left ventricular volumes between sestamibi and ^{82}Rb at stress and at rest increased with increasing volumes. This trend could be explained by the presence of reversible perfusion abnormalities on both sestamibi and ^{82}Rb. However, these differences had only a limited effect on the LVEF. Moreover, Bland-Altman analysis showed that there was no trend or bias in LVEF between the sestamibi and ^{82}Rb images at stress. In addition, Bland-Altman analysis showed that with increasing perfusion abnormalities (SSS and SRS) the sestamibi perfusion images had higher values as compared with the ^{82}Rb images. By contrast the reversibility index (SDS) had lower scores on the sestamibi perfusion images with increasing mean values as compared with the ^{82}Rb images.

In general PET myocardial perfusion provides better quality images and has better diagnostic properties (higher sensitivity and specificity) compared with SPECT myocardial perfusion studies [10, 11]. However, a major limitation of these comparative studies is that they were performed in different patient cohorts or at different time points [10]. Although the body mass index in these studies was comparable between populations, patients' body habitus may have been different between the studied cohorts. Also, the presence of

Table 3 Mean values and standard deviation of the functional parameters compared according to normal or abnormal myocardial perfusion

Parameter	Sestamibi		^{82}Rb		*p*-value	
	Normal ($n = 144$) (SSS ≤ 3)	Abnormal ($n = 77$) (SSS ≥ 3)	Normal ($n = 135$) (SSS ≤ 3)	Abnormal ($n = 86$) (SSS ≥ 3)	Normal (SPECT vs PET)	Abnormal (SPECT vs PET)
Rest LVEF (%)	61.35 ± 13.76	48.45 ± 14.96	58.37 ± 16.12	50.16 ± 18.13	0.010	0.974
Stress LVEF (%)	62.29 ± 14.31	47.84 ± 15.19	64.95 ± 14.80	53.71 ± 16.86	≤0.001	≤0.001
Rest EDV (mL)	84.46 ± 36.12	125.44 ± 74.09	80.36 ± 34.35	99.61 ± 54.45	≤0.001	≤0.001
Stress EDV (mL)	85.25 ± 39.87	125.88 ± 73.96	89.84 ± 36.27	110.08 ± 55.80	0.049	0.006
Rest ESV (mL)	35.99 ± 25.81	72.34 ± 67.47	35.49 ± 25.79	55.76 ± 50.74	0.014	≤0.001
Stress ESV (mL)	36.29 ± 30.54	73.38 ± 66.28	34.76 ± 26.38	56.21 ± 50.70	0.097	≤0.001

SSS summed stress score, *Rest LVEF* left ventricular ejection fraction at rest, *Stress LVEF* stress left ventricular ejection fraction, *Rest EDV* end diastolic volume at rest, *Stress EDV* stress end diastolic volume, *Rest ESV* end systolic volume at rest, *Stress ESV* stress end systolic volume

comorbidities could result in referral bias between the different modalities. And last but not least, sometimes perfusion images were compared using different types of stress [4]. These issues combined could explain, at least in part, the previously reported differences between PET and SPECT studies [4, 10].

We found that differences in left ventricular volumes between sestamibi and ^{82}Rb could be independently predicted by the presence of reversible perfusion abnormalities. However, the negative slope of the regression coefficient counterintuitively suggests that with increasing amounts of reversible perfusion abnormalities the differences in volume between sestamibi and ^{82}Rb decline. At the time of acquisition, myocardial distribution and uptake of the tracer reflect perfusion at the time of tracer injection (i.e., exercise, pharmacologically induced stress, or rest). However, the acquisition of left ventricular function reflects real time. In patients with stress-induced ischemia, left ventricular function may be impaired temporarily [12]. The time course for the resolution of postischemic left ventricular dysfunction is variable [13–16]. Postischemic reversible contractile dysfunction known as myocardial stunning is common in patients with coronary artery disease [17–20]. It is, therefore, possible that LVEF assessed after stress may not reflect basal LVEF [21, 22]. It is also very likely that the resolution of the postischemic stunning is related with the amount of myocardial ischemia (i.e. larger amounts of ischemia result in longer time before postischemic stunning has been resolved). Therefore, the sequential imaging (i.e. ^{82}Rb followed by sestamibi) after a single stress test may have demonstrated larger differences in left ventricular volumes between sestamibi and ^{82}Rb with smaller amounts of ischemia in this study.

The relative small differences in perfusion abnormalities showed larger scores for both sestamibi SSS and SRS perfusion images with increasing mean values when compared to ^{82}Rb images. However, the reversibility index (SDS) showed a pattern with lower scores for the sestamibi perfusion images with increasing mean values when compared to the ^{82}Rb images. This means that although the sestamibi images are scored more severely with increasing perfusion abnormalities, this did not result in more pronounced amounts of ischemia. The contrast (difference between stress and rest) on the ^{82}Rb PET images was more pronounced leading to larger amounts of visually assessed ischemic myocardium. In part, these differences between sestamibi and ^{82}Rb can be explained by the intrinsic higher quality of the PET images. This is in line with the observation of Flotats et al. that ^{82}Rb PET offers improved image quality most likely leading to interpretive confidence and interreader agreement [4].

On group level there were no statistical significant differences in the frequency of normal or abnormal perfusion images. However, looking at the individual patient level classification changed in 18% when any difference between the two techniques was considered and in 14% when the differences in SSS between the two techniques was ≥2. The clinical implications of these individual differences could be significant and impact patients' clinical outcome. However, the true value of these discrepancies are best appreciated in relation clinical outcome. In addition there were differences in volumes between sestamibi SPECT and ^{82}Rb PET for both normal and abnormal perfusion images. These differences in volume also resulted in statistical significant but relatively small differences in LVEF.

In this study, the use of a single stress test for both imaging modalities minimized physiological variables, including the day-to-day circadian variations, medication and caffeine blood levels that could interfere with the patient's hemodynamic response to dipyridamole. The design made a real head-to head comparison possible. We realize that there are alternatives to dipyridamole as a vasodilator (i.e. adenosine, regadenoson) [23] and that more than 50% of patients develop side effects with dipyridamole (flushing, chest pain, headache,

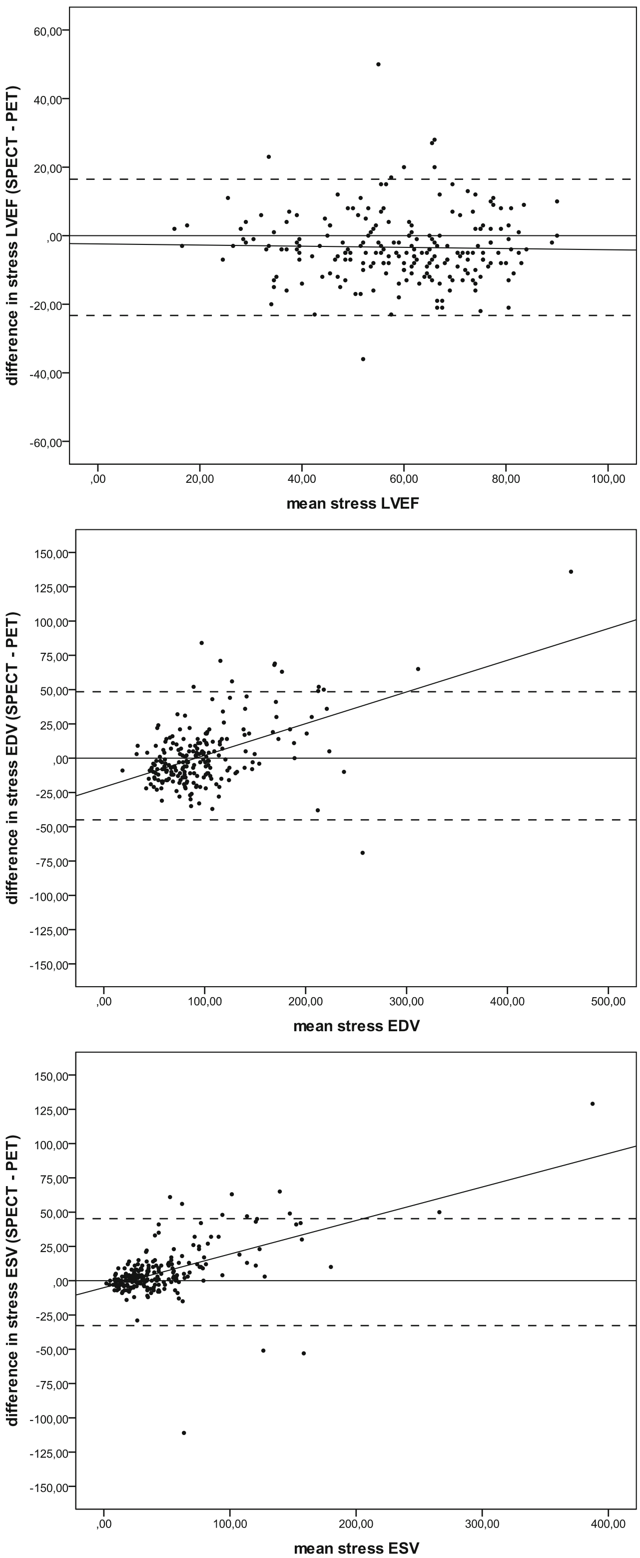

Fig. 3 Bland-Altman plots showing the difference between the LVEF (**a**), EDV (**b**), and ESV (**c**) plotted against the mean values of these parameters assessed on the sestamibi SPECT and ^{82}Rb PET images post-stress. Differences were calculated as sestamibi SPECT minus ^{82}Rb PET. The *dashed lines* indicate the 95% limits of agreement of the mean difference and the *solid angular lines* indicate the regression line

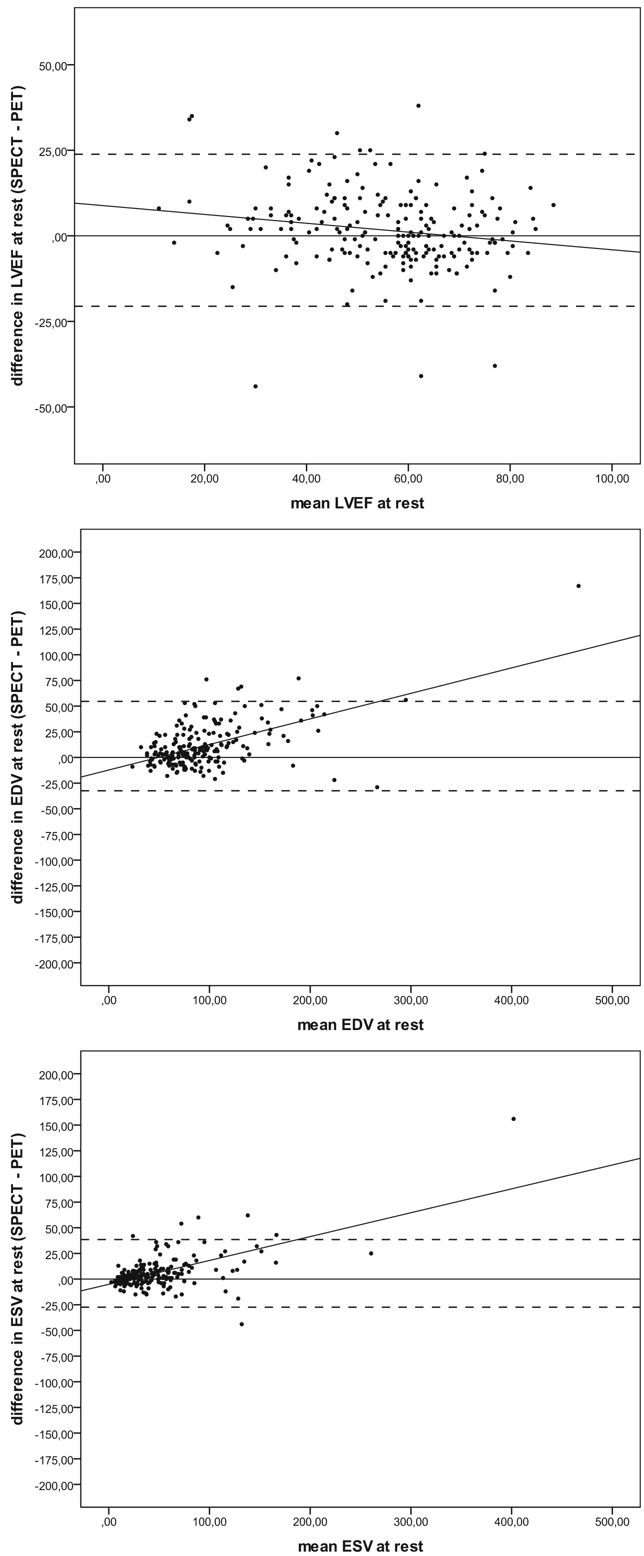

Fig. 4 Bland-Altman plots showing the difference between the LVEF (**a**), EDV (**b**), and ESV (**c**) plotted against the mean values of these parameters assessed on the sestamibi SPECT and ^{82}Rb PET images at rest. Differences were calculated as sestamibi SPECT minus ^{82}Rb PET. The *dashed lines* indicate the 95% limits of agreement of the mean difference and the *solid angular lines* indicate the regression line

Table 4 Multivariate regression analysis to determine independent predictors for the differences in left ventricular volumes between stress sestamibi and ^{82}Rb MPI

Variables	Coefficient *b*	Standard error *b*	*p*-value
Independent predictors for differences in stress EDV			
Constant	17.727	9.007	0.054
Sestamibi SRS	1.709	0.215	<0.001
^{82}Rb SDS	−0.991	0.366	0.007
Age	−0.296	1.33	0.027
Goodness-of-fit of the model	Adjusted R^2		*p*-value
	0.236		<0.001
Independent predictors for differences in stress ESV			
Constant	21.251	7.706	0.006
^{82}Rb SRS	2.026	0.283	<0.001
Age	−0.282	0.114	0.014
Sestamibi SDS	−1.024	0.509	0.046
Goodness-of-fit of the model	Adjusted R^2		*p*-value
	0.202		<0.001

SRS summed rest score, *SDS* summed difference score, *Stress EDV* stress end diastolic volume, *Stress ESV* stress end systolic volume

dizziness, or hypotension). However, the frequency of these side effects is lower than that seen with adenosine. On the other hand these side effects last longer (15–25 min) and theophylline or aminophylline (125–250 mg, i.v.) may be required [24]. But the incidence of high-degree AV and SA blocks with dipyridamole is lower than that observed with adenosine (2%) [25]. Summarizing, although dipyridamole is not the most ideal vasodilator it has been proven to be relatively safe for clinical use.

Knowledge on repeatability and reproducibility are essential to have a better understanding of the used parameters (i.e. perfusion abnormalities and estimates of left ventricular function). Although these types of analyses were not performed in the present study there is some data available on this subject. Johansen et al. showed that in a group of consecutive male patients with stable angina pectoris interpretive agreement between two independent observers of sestamibi stress and rest images was good to excellent. However, the agreement for

Table 5 Multivariate regression analysis to determine independent predictors for the differences in left ventricular volumes and function between sestamibi and ^{82}Rb MPI at rest

Variables	Coefficient *b*	Standard error *b*	*p*-value
Independent predictors for differences in EDV at rest			
Constant	6.863	1.585	<0.001
Sestamibi SRS	1.713	0.197	<0.001
^{82}Rb SDS	−0.959	0.338	0.005
Goodness-of-fit of the model	Adjusted R^2		*p*-value
	0.261		<0.001
Independent predictors for differences in ESV at rest			
Constant	1.957	1.172	0.096
Sestamibi SRS	1.833	0.146	<0.001
^{82}Rb SDS	−0.664	0.250	0.008
Goodness-of-fit of the model	Adjusted R^2		*p*-value
	0.296		<0.001
Independent predictors for differences in LVEF at rest			
Constant	−12.596	4.824	0.01
Age	0.226	0.071	0.002
^{82}Rb SRS	−0.359	0.174	0.04
Goodness-of-fit of the model	Adjusted R^2		*p*-value
	0.056		0.04

SRS summed rest score, *SDS* summed difference score, *Rest EDV* end diastolic volume at rest, *Rest ESV* end systolic volume at rest segmental scoring was moderate to good [26]. In another study, quantitative analysis of ^{99m}Tc-sestamibi myocardial perfusion SPECT was compared with experienced observers. As expected the operator independent quantification method showed no variation in outcome. The quantification method showed a moderate agreement with individual observers and a panel analysis for size and severity of perfusion abnormalities. In addition, the automatic quantification had a similar ability to assign perfusion abnormalities to the diseased coronary artery as compared to an expert panel [27]. Comparison of three commercially available software packages for measuring left ventricular perfusion and function by gated SPECT myocardial perfusion imaging showed significant differences in measuring perfusion abnormalities as well as LV function, and more importantly in defining small, moderate, or large ischemic burden [28]. Similar data for semi-quantitative analysis of ^{82}Rb PET are not available, but it is most likely that for ^{82}Rb PET these values are in the same range as for sestamibi SPECT.

A strong point of this study is that the population studied consisted of patients routinely evaluated for the presence or extent of CAD irrespective of a clinical subset. The data, therefore, most likely reflect real clinical life.

This study is limited by the fact that quantitative and angiographic data were only available in a minority of the subjects included, making these data not useful for the present analyses. This implies that the lack quantification of myocardial blood flow, that must be regarded as state-of-the-art, could not be used as reference. This lack of functional and anatomical data hampered calculation and comparison of diagnostic accuracy (i.e. sensitivity, specificity, negative and positive predictive values). However, the choice of an anatomical gold standard may reduce the real value of functional tests like SPECT or PET myocardial perfusion imaging and this leads to greater perceived accuracy for the anatomical tests [29, 30]. However when SPECT and PET myocardial perfusion imaging are directly compared for their diagnostic accuracy to detect angiographically assessed coronary artery disease, a meta-analysis including 11,862 patients showed a higher sensitivity of ^{82}Rb studies [31]. In addition, in the present study, data on regional wall motion were not compared. Despite these limitations the outcome of the study still seems valid as the objective of this study was to directly compare LV functional parameters obtained from sestamibi and ^{82}Rb examinations in a clinical setting.

Clinical implications

Apart from the technical differences, our data indicate that there are some differences between sestamibi and ^{82}Rb studies that may imply differences in diagnostic and prognostic outcome, both in patients with suspected or established coronary artery disease.

Conclusion

There are differences in left ventricular volumes between sestamibi and ^{82}Rb MPI that increase with increasing volumes. However, these differences did only marginally affect LVEF between sestamibi and ^{82}Rb. In clinical practice these results should be taken into account when comparing functional derived parameters between sestamibi and ^{82}Rb MPI.

Acknowledgements The authors kindly acknowledge Luis T. Gonçalves, Rosa C. de Abreu Silva and the nuclear medicine staff for helping with the examinations; Mrs. Renata Do Val and Ruth Mello Diniz Ribeiro for helping with data collection.

Compliance with ethical standards

Funding This study was supported in part by FAPESP (Fundação de Amparo à Pesquisa do Estado de São Paulo) research grant number 2010/51100-7 and Fundação Zerbini.

Conflict of interest None of the authors has a conflict of interest.

Ethical approval All procedures performed in studies involving human participants were in accordance with the ethical standards of the institutional and/or national research committee and with the 1964 Helsinki declaration and its later amendments or comparable ethical standards.

Informed consent Informed consent was obtained from all individual participants included in the study.

References

1. Slomka PJ, Dey D, Duvall WL, Henzlova MJ, Berman DS, Germano G. Advances in nuclear cardiac instrumentation with a view towards reduced radiation exposure. Curr Cardiol Rep. 2012;14(2):208–16.
2. Wells RG, Soueidan K, Timmins R, Ruddy TD. Comparison of attenuation, dual-energy-window, and model-based scatter correction of low-count SPECT to 82Rb PET/CT quantified myocardial perfusion scores. J Nucl Cardiol. 2013;20(5):785–96.
3. Tout D, Davidson G, Hurley C, Bartley M, Arumugam P, Bradley A. Comparison of occupational radiation exposure from myocardial perfusion imaging with Rb-82 PET and Tc-99m SPECT. Nucl Med Commun. 2014;35(10):1032–7.
4. Flotats A, Bravo PE, Fukushima K, Chaudhry MA, Merrill J, Bengel FM. (8)(2)Rb PET myocardial perfusion imaging is superior to (9)(9)mTc-labelled agent SPECT in patients with known or suspected coronary artery disease. Eur J Nucl Med Mol Imaging. 2012;39(8):1233–9.

5. Go RT, Marwick TH, MacIntyre WJ, Saha GB, Neumann DR, Underwood DA, et al. A prospective comparison of rubidium-82 PET and thallium-201 SPECT myocardial perfusion imaging utilizing a single dipyridamole stress in the diagnosis of coronary artery disease. J Nucl Med. 1990;31(12):1899–905.
6. Hsiao E, Ali B, Blankstein R, Skali H, Ali T, Bruyere Jr J, et al. Detection of obstructive coronary artery disease using regadenoson stress and 82Rb PET/CT myocardial perfusion imaging. J Nucl Med. 2013;54(10):1748–54.
7. Kay J, Dorbala S, Goyal A, Fazel R, Di Carli MF, Einstein AJ, et al. Influence of sex on risk stratification with stress myocardial perfusion Rb-82 positron emission tomography: results from the PET (Positron Emission Tomography) Prognosis Multicenter Registry. J Am Coll Cardiol. 2013;62(20):1866–76.
8. Maddahi J, Packard RR. Cardiac PET perfusion tracers: current status and future directions. Semin Nucl Med. 2014;44(5):333–43.
9. Cerqueira MD, Weissman NJ, Dilsizian V, Jacobs AK, Kaul S, Laskey WK, et al. Standardized myocardial segmentation and nomenclature for tomographic imaging of the heart. A statement for healthcare professionals from the Cardiac Imaging Committee of the Council on Clinical Cardiology of the American Heart Association. Circulation. 2002;105(4):539–42.
10. Bateman TM, Heller GV, McGhie AI, Friedman JD, Case JA, Bryngelson JR, et al. Diagnostic accuracy of rest/stress ECG-gated Rb-82 myocardial perfusion PET: comparison with ECG-gated Tc-99m sestamibi SPECT. J Nucl Cardiol. 2006;13(1):24–33.
11. Mc Ardle BA, Dowsley TF, de Kemp RA, Wells GA, Beanlands RS. Does rubidium-82 PET have superior accuracy to SPECT perfusion imaging for the diagnosis of obstructive coronary disease?: A systematic review and meta-analysis. J Am Coll Cardiol. 2012;60(18):1828–37.
12. Brown TL, Merrill J, Volokh L, Bengel FM. Determinants of the response of left ventricular ejection fraction to vasodilator stress in electrocardiographically gated (82)rubidium myocardial perfusion PET. Eur J Nucl Med Mol Imaging. 2008;35(2):336–42.
13. Ambrosio G, Betocchi S, Pace L, Losi MA, Perrone-Filardi P, Soricelli A, et al. Prolonged impairment of regional contractile function after resolution of exercise-induced angina. Evidence of myocardial stunning in patients with coronary artery disease. Circulation. 1996;94(10):2455–64.
14. Nixon JV, Brown CN, Smitherman TC. Identification of transient and persistent segmental wall motion abnormalities in patients with unstable angina by two-dimensional echocardiography. Circulation. 1982;65(7):1497–503.
15. Rozanski A, Berman D, Gray R, Diamond G, Raymond M, Prause J, et al. Preoperative prediction of reversible myocardial asynergy by postexercise radionuclide ventriculography. N Engl J Med. 1982;307(4):212–6.
16. Rozanski A, Elkayam U, Berman DS, Diamond GA, Prause J, Swan HJ. Improvement of resting myocardial asynergy with cessation of upright bicycle exercise. Circulation. 1983;67(3):529–35.
17. Bolli R. Mechanism of myocardial "stunning". Circulation. 1990;82(3):723–38.
18. Bolli R, Marban E. Molecular and cellular mechanisms of myocardial stunning. Physiol Rev. 1999;79(2):609–34.
19. Braunwald E, Kloner RA. The stunned myocardium: prolonged, postischemic ventricular dysfunction. Circulation. 1982;66(6): 1146–9.
20. Heyndrickx GR, Millard RW, McRitchie RJ, Maroko PR, Vatner SF. Regional myocardial functional and electrophysiological alterations after brief coronary artery occlusion in conscious dogs. J Clin Invest. 1975;56(4):978–85.
21. Johnson LL, Verdesca SA, Aude WY, Xavier RC, Nott LT, Campanella MW, et al. Postischemic stunning can affect left ventricular ejection fraction and regional wall motion on post-stress gated sestamibi tomograms. J Am Coll Cardiol. 1997;30(7): 1641–8.
22. Verberne HJ, Dijkgraaf MG, Somsen GA, van Eck-Smit BL. Stress-related variations in left ventricular function as assessed with gated myocardial perfusion SPECT. J Nucl Cardiol. 2003;10(5):456–63.
23. Cullom SJ, Case JA, Courter SA, McGhie AI, Bateman TM. Regadenoson pharmacologic rubidium-82 PET: a comparison of quantitative perfusion and function to dipyridamole. J Nucl Cardiol. 2013;20(1):76–83.
24. Verberne HJ, Acampa W, Anagnostopoulos C, Ballinger J, Bengel F, De Bondt P, et al. EANM procedural guidelines for radionuclide myocardial perfusion imaging with SPECT and SPECT/CT: 2015 revision. Eur J Nucl Med Mol Imaging. 2015;42(12):1929–40.
25. Lette J, Tatum JL, Fraser S, Miller DD, Waters DD, Heller G, et al. Safety of dipyridamole testing in 73,806 patients: the Multicenter Dipyridamole Safety Study. J Nucl Cardiol. 1995;2(1):3–17.
26. Johansen A, Gaster AL, Veje A, Thayssen P, Haghfelt T, Holund-Carlsen PF. Interpretive intra- and interobserver reproducibility of rest/stress 99Tcm-sestamibi myocardial perfusion SPECT in a consecutive group of male patients with stable angina pectoris before and after percutaneous transluminal angioplasty. Nucl Med Commun. 2001;22(5):531–7.
27. Verberne HJ, Habraken JB, van Royen EA, van Buul MM T, Piek JJ, van Eck-Smit BL. Quantitative analysis of 99Tcm-sestamibi myocardial perfusion SPECT using a three-dimensional reference heart: a comparison with experienced observers. Nucl Med Commun. 2001;22(2):155–63.
28. Ather S, Iqbal F, Gulotta J, Aljaroudi W, Heo J, Iskandrian AE, et al. Comparison of three commercially available softwares for measuring left ventricular perfusion and function by gated SPECT myocardial perfusion imaging. J Nucl Cardiol. 2014;21(4):673–81.
29. Neglia D, Rovai D, Caselli C, Pietila M, Teresinska A, Aguade-Bruix S, et al. Detection of significant coronary artery disease by noninvasive anatomical and functional imaging. Circ Cardiovasc Imaging. 2015;8(3).
30. Reyes E, Underwood SR. Coronary anatomy and function: a story of Yin and Yang. Eur Heart J Cardiovasc Imaging. 2015;16(8):831–3.
31. Parker MW, Iskandar A, Limone B, Perugini A, Kim H, Jones C, et al. Diagnostic accuracy of cardiac positron emission tomography versus single photon emission computed tomography for coronary artery disease: a bivariate meta-analysis. Circ Cardiovasc Imaging. 2012;5(6):700–7.